



The Role of microRNA-133 in Hemocyte Proliferation and Innate Immunity of *Scylla paramamosain*

Yunfei Zhang, Yongyong Lai, Xiujuan Zhou and Fei Zhu*

Key Laboratory of Applied Technology on Green-Eco-Healthy Animal Husbandry of Zhejiang Province, College of Animal Science and Technology, College of Veterinary Medicine, Zhejiang Agriculture and Forestry University, Hangzhou, China

MicroRNAs (miRNAs) are important signaling regulators that are involved in regulating the innate immunity of crustacean. However, few studies focus on the role of crustacean miRNAs in the cellular immunity have been reported. In this study, we showed that the expression of miR-133 was significantly up-regulated in the mud crab *Scylla paramamosain* after infection by white spot syndrome virus (WSSV) or *Vibrio parahaemolyticus*. The anti-miRNA oligonucleotide AMO-miR-133 was used to knock down miR-133 expression in *S. paramamosain*. The number of WSSV copies increased significantly in WSSV-infected crabs after miR-133 knockdown. Knockdown of miR-133 also enhanced the mortality rates of WSSV-infected and *V. parahaemolyticus*-infected mud crabs, and it significantly enhanced the expression of the astakine, which was confirmed by real-time quantitative PCR and western blot analysis. The data also indicate that miR-133 may affect hemocyte proliferation in *S. paramamosain* by regulating *astakine* expression. miR-133 Knockdown enhanced the apoptosis or phagocytosis of crab hemocytes, and increased the mortality of mud crabs after WSSV or *V. parahaemolyticus* infection. These results indicate that miR-133 is involved in the host immune response to WSSV and *V. parahaemolyticus* infection in mud crabs. Taken together, our research provides new insights for the control of viral or vibrio diseases in *S. paramamosain*.

Keywords: microRNA-133, hemocyte proliferation, innate immunity, *Scylla paramamosain*, white spot syndrome virus, *Vibrio parahaemolyticus*

OPEN ACCESS

Edited by:

Chaofeng Han,
Second Military Medical University,
China

Reviewed by:

Hengwei Deng,
Sun Yat-sen University, China
Ying Huang,
Hohai University, China

*Correspondence:

Fei Zhu
zhufei@zafu.edu.cn

Specialty section:

This article was submitted to
Molecular Innate Immunity,
a section of the journal
Frontiers in Immunology

Received: 10 November 2021

Accepted: 28 December 2021

Published: 27 January 2022

Citation:

Zhang Y, Lai Y, Zhou X and Zhu F
(2022) The Role of microRNA-133 in
Hemocyte Proliferation and Innate
Immunity of *Scylla paramamosain*.
Front. Immunol. 12:812717.
doi: 10.3389/fimmu.2021.812717

INTRODUCTION

MicroRNAs (miRNAs) are highly conserved endogenous small non-coding RNAs, which regulate gene expression at post-transcriptional levels and protein synthesis in eukaryotes (1). miRNAs play major roles in regulating biological processes, including cell proliferation, cell differentiation, apoptosis, DNA replication, and signal transduction (2–4). In crustaceans, miRNAs have been reported to be involved in the immune response to pathogen infections. For example, the expression level of miR-146 and miR-132 were significantly up-regulated in *Vibrio parahaemolyticus*-infected mud crabs (*Scylla paramamosain*) (5). The expression level of some miRNAs changed in *V. parahaemolyticus*-infected shrimp (*Litopenaeus vannamei*), including 47 miRNAs that were up-regulated and 36 miRNAs that were down-regulated (6). Similarly, Zhu et al. identified more than 50 kinds of miRNAs that responded to *Vibrio alginolyticus* infection in *Marsupenaeus*

japonicus, and the expression levels of some of them were up-regulated (7). These reports indicate that crustacean miRNAs are associated with the process of *Vibrio* infection and may play an important role in regulation of innate immunity.

Furthermore, some researchers reported that the overexpression of miR-7 and miR-217 in the Chinese mitten crab (*Eriocheir sinensis*) was beneficial to white spot syndrome virus (WSSV) infection (8, 9). In contrast, some microRNAs in the Chinese white shrimp (*Fenneropenaeus chinensis*) were found to participate in the host response to challenge with WSSV. In another study, researchers found that the expression of 10 miRNAs in *F. chinensis* was up-regulated post-WSSV infection (10). Thus, miRNAs may also play a major role in the crustacean response to viral infection.

As one of the most important mud crab species in southeastern China, *S. paramamosain* has high economic value (11). Currently, the crab breeding industry in China is undergoing vigorous development and the mud crab aquaculture production exceeded 161 thousand tons in 2019 (12). WSSV and *V. parahaemolyticus* are two common pathogens that can infect mud crabs. However, to date, an effective method to prevent and treat WSSV and *V. parahaemolyticus* infection does not exist. Some reports have shown that hemocytes play an important role in cellular immune defense, and they can secrete several immune-related cytokines that participate in the humoral immune response (13–15). The miR-133 was first cloned and identified from mammalian muscle tissue in 2003 (16). Several studies have shown that miR-133 can significantly affect the proliferation of skeletal muscle and regeneration of myocardium in mice (17, 18), and its overexpression can significantly inhibit the proliferation of mouse vascular smooth muscle cells (17). Biological studies have confirmed that miR-133 overexpression can inhibit the proliferation of cancer cells (19, 20). Moreover, miR-133 is widely involved in the proliferation and differentiation of cardiomyocytes (21). And miR-133 can decrease cardiomyocyte apoptosis by mediating the expression of apoptosis-related genes in the hearts of mice (22).

In summary, miR-133 plays a positive role in regulating cell proliferation and apoptosis. The miR-133 was found to be up-regulated in hemocytes of *S. paramamosain* when response to WSSV and *V. parahaemolyticus* infection (23, 24). Thus, we propose that miR-133 may have similar biological functions in *S. paramamosain*. In addition, Non-specific immunity played a vital role in the defense of crustaceans against viruses, among which cellular immune response is an important part, especially because they rely on innate immunity to defend against viral infection (25). WSSV and *V. parahaemolyticus* are the main pathogens of mud crabs, and they cause great losses to the aquaculture industry. In this study, we evaluated the role of miR-133 on astakine (a hematopoietic cytokine in crustaceans) expression and cell proliferation and its effects on innate immunity and microbe pathogen infection in *S. paramamosain* **Table 1**.

METHODS AND MATERIALS

Preparation of Crabs and Pathogens

Healthy *S. paramamosain* (average weight 90–95 g, average carapace width 8.0 cm and carapace length 5.8 cm) were

purchased from a market in Hangzhou, China, and acclimated in the aerated seawater at 25°C for 3–4 days before being used in the experiments. Three crabs were randomly selected to detect by a mentioned method described (26, 27) to ensure that the crabs were healthy before the experiments. WSSV used in this study was extracted from tissues of infected crayfish (*Procambarus clarkii*) following a previously described method (26). *V. parahaemolyticus* (ATCC 17802) was stored in an ultra-low temperature freezer in the laboratory and cultured in 2216E medium at 28°C. *V. parahaemolyticus* was collected in 1 ml phosphate buffered saline (PBS), washed three times with PBS, and used to infect the crabs following a previously described method (27).

Silencing of *S. paramamosain* miR-133, WSSV or *V. parahaemolyticus* Challenge, and Survival Analysis

The sequence of *S. paramamosain* miR-133 was (5'-GCCUCG UUUAGCUGGCUGAAUCCGGGCCAAAUUGUUUAUUCUAU G A G C A G C A U U G G U C C C C U U C A A C C A G C UGUAGUUGGCAUUCUGAGCAAC-3'). The sequence of miR-133 was (5'-TTGGTCCCCCTTCAACCAGCTGT-3'). To knockdown crab miR-133 expression, the anti-miRNA-133 oligonucleotide (AMO-miR-133: 5'-AGCTGGTTGAAGGGGACC-3') was injected into the crab at a dose of 0.5 nmol/crab. As a control, the sequence of AMO-miR-133 was scrambled, and shown as AMO-miR-133-scramble. The experiment divided into two parts: immune index detection and survival analysis. For the first part, experimental mud crabs were distributed randomly into seven groups (3 crabs/group), with three replicates per group. Five groups were treated by intramuscular injection of 100 μ L of PBS (control), AMO-miR-133 (0.5 nmol/crab), AMO-miR-133-scramble (0.5 nmol/crab), WSSV (10^6 copies/mL), or *V. parahaemolyticus* (10^5 CFU/mL), respectively. The other two groups were injected with a 100 μ L mixture of AMO-miR-133 (0.5 nmol/crab) and either (WSSV (10^6 copies/mL) or *V. parahaemolyticus* (10^5 CFU/mL), respectively. At 12 h after the first injection, the anti-miRNA-133 oligonucleotide was injected into each crab.

The experimental grouping for survival analysis was the same as that described above, except AMO-miR-133-scramble group. Each group consisted of 10 crabs, and they were injected with the same doses as described above. Water in each group was replaced with fresh seawater every 24 h, at which time we recorded the number of dead crabs.

RNA Extraction and cDNA Synthesis

The miRNA was extracted from healthy, WSSV-infected or *V. parahaemolyticus*-infected mud crabs hemocytes. And the miRNA of AMO-miR-133-scramble-treated or AMO-miR-133-treated *S. paramamosain* was also extracted from hemocytes. The extractions were performed following the manufacturer's instructions for the miPure Cell/Tissue miRNA kit (Vazyme, Jiangsu, China). The collected miRNA samples were stored at -70°C prior to use. The miRNA first strand cDNA synthesis kit (Vazyme) was used to synthesize cDNA according to the manufacturer's instruction. The PCR program was 5 min at 25°C, 15 min at 50°C, and 5 min at 85°C.

TABLE 1 | Universal and specific primers used in this study.

Primer Name	Primer Sequence (5' to 3')	Purpose
GAPDH-F	ACCTCACCAACTCCAACAC	for GAPDH expression
GAPDH-R	CATTACAGCCACAACCT	
β -actin-F	ACCACTGCCGCCCTCATCCTC	for β -actin expression
β -actin-R	CGGAACCTCTCGTTGCCAATGG	
STAT-F	GACTTCACTAACTTCAGCCTCG	for STAT expression
STAT-R	GAGCTGAGTCTGTCTTAATGTTATCC	
Astakine-F	CACCAGGTAGTAATCAGGGA	for Astakine expression
Astakine-R	AAGGCACCCAACTTCTCA	
MCM7-F	ACTTTGCTAACGCCAATCCAC	for MCM7 expression
MCM7-R	CTAGGCTGTCATCGACGAACC	
proPO-F	ATGAAAGAGGAGTGGAGATG	For proPO expression
proPO-R	GTGATGGATGAGGAGGTG	
Myosin-F	GCCGAGATAAGTGTAGAGGAA	For Myosin expression
Myosin-R	AGTGGGGTTCTGTCCAAG	
Toll-like receptor-F	TGTTGCCAGAGCAGAAGGT	forToll-like receptor expression
Toll-like receptor-R	TTCCGTGAATGAACGAAGG	
Relish-F	CAGGTACACCTTTGTGACCCG	for Relish expression
Relish-R	CCTTCTACTTAGGGCATTTCG	
CAP-F	GCCTTTACCAACGGCTTCTTC	for Crustin antimicrobial peptide expression
CAP-R	ACAGTAGCTTCCATGCAATTC	
WSSV-F	TATTGTCTCTCCTGACGTAC	for WSSV expression
WSSV-R	CACATTCTCAGAGTCTAC	
AMO-miR-133	AGCTGGTTGAAGGGGACC	for miR-133 knockdown
AMO-miR-133 scrambled	CTAGGAGTGAAGGCGTC	
U6-F	CGCTTCGGCAGCAGATATA	for U6 expression
U6-R	TTCACGAATTTGCGTGTGTCAT	
RT-miR-133	GTGCTATCCAGTGCAGGGTCCGAGGTATTGCACTGGATACGACACAGCT	for reversing miR-133
miR-133-F	CGTTGGTCCCCTTCAACC	for miR-133 expression
miR-133-R	AGTGCAGGGTCCGAGGTATT	

The total RNA from healthy or AMO-miR-133-treated *S. paramamosain* hemocytes was extracted using Trizol reagent according to the manufacturer's instructions, and cDNA was synthesized using the PrimeScript RT reagent kit (TaKaRa, Dalian, China).

Real-Time Quantitative PCR (RT-qPCR)

To monitor gene expression changes in *S. paramamosain* treated with AMO-miR-133 at 24 h post-treatment, three samples of *S. paramamosain* hemocytes were collected for each treatment and the control. The total RNA was extracted from the collected samples and cDNA was synthesized. Samples were analyzed using RT-qPCR following previously described methods (28). The PCR program was 30 s at 95°C; 45 cycles of 5 s at 95°C, 30 s at 60°C; 60 s at 95°C; 30 s at 55°C, and 30 s at 95°C. GAPDH was used as the internal control (28–30). The primers used for RT-qPCR were listed in **Supplementary Table 1**. The data for expression of each gene were evaluated using the $2^{-\Delta\Delta Ct}$ method (28).

WSSV Copy Analysis

Five healthy *S. paramamosain* from the WSSV group were injected with WSSV (10^6 copies/mL) diluted in 100 μ L of PBS, and five mud crabs injected with 100 μ L of PBS served as the control group. *S. paramamosain* in the WSSV + AMO-miR-133 group were injected with a 100 μ L mixture of AMO-miR-133 (0.5 nmol/crab) and WSSV (10^6 copies/mL). Twelve hours after the first injection, the anti-miRNA-133 oligonucleotide was injected into the crabs. Hemocyte samples from three

individuals from each group were collected at different times post-injection (0, 24, 48, 72 h) and we used absolute RT-qPCR to monitor WSSV copy numbers in *S. paramamosain* hemocytes.

The program was as follows: 1 cycle for 4 min at 50°C, followed by 45 cycles of 45 s at 95°C, 45 s at 52°C, and 45 s at 72°C. We collected hemocytes from *S. paramamosain* at different times post-challenge. Hemocyte DNA was extracted using a DNA isolation kit (Generay, Shanghai, China) following the manufacturer's instructions. According to a previously described method (31), the viral load in 200 ng samples of *S. paramamosain* hemocyte DNA was then calculated. We used VP28 protein specific primers (5'-TTGGTTTCAGCCCCGA-GATT-3' and 5'-CCTTGGTCAGCCCCCTTGA-3') and TaqMan fluorescent probe (5'-FAM-TGCTGCCGTCTCCAA-TAMRA-3') to measure the number of WSSV genomic copies.

Superoxide Dismutase (SOD), Phenoloxidase (PO), and Catalase (CAT) Activities and Total Hemocyte (THC) Counts

SOD and PO activities were measured following a previously described method (31), as was serum CAT activity (26). The THC counts were assayed using a Burkner hemocytometer (Erma, Tokyo, Japan). Measurements were made following a previously described method (32).

Cell Culture, AMO-miR-133 Transfection, and Reactive Oxygen Species (ROS) Analysis

S. paramamosain hemocytes were collected and cultured following a previously described method (28). They were

cultured at 28°C for 24 h, and then Lipofectamine 2000 (Invitrogen, USA) was used to transfect AMO-miR-133 (5 pmol/each well) into the cells. The PBS group served as the control. The cells were cultured in 96-well plates for different amounts of time (24, 36, and 48 h), and hemocyte proliferation levels were measured at each time point (28).

For ROS analysis, hemocytes were collected and cultured as described above. At 24 h after transfection, we measured the generated ROS in the hemocytes of the AMO-miR-133 group and the control group following a previously described method (33). We used a fluorescence labeling instrument (BioTek, Winooski, VT, USA) to measure the wavelengths of excitation at 488 nm and emission at 525 nm. The generation of ROS in cells was observed under an inverted fluorescence microscope (Nikon, Tokyo, Japan).

Phagocyte Rate Counting by Flow Cytometry

V. parahaemolyticus was cultured at 37°C for 12 h on a constant temperature shaker, followed by harvesting using centrifuge at 4000 rpm for 10 min at 4°C and resuspension in PBS. Samples were placed in a water bath at 80°C for 60 min and then incubated with 5 mg/mL fluorescent isothiocyanate (FITC; Sigma, USA) at 25°C for 90 min. PBS was used to wash labelled *V. parahaemolyticus* until the supernatant was clear. WSSV samples were labelled following a previously described method (34).

The hemocyte samples were collected from each group and placed in pre-cooled ACD-B (pH 4.6; citric acid 0.96 g/200 mL; sodium citrate 2.64 g/200 mL; glucose 2.94 g/200 mL; NaCl 0.24 g/200 mL) at a ratio of 1:1. The samples were centrifuged at 300 g x 5 min at 4°C to collect hemolymph cells.

Apoptosis Analysis of Crab Hemocytes

At 24 h after injection with AMO-miR-133, the pathogen, or their mixture, hemocytes were collected from each group, and the apoptosis analysis was performed following a previous method (34). Cell apoptosis of each sample was examined by flow cytometry, and the cells in quadrant 4 with low propidium iodide (PI) and high annexin V staining was considered to be apoptotic.

Western Blot

The hemocyte samples from each group were mixed with anticoagulant solution at a 1:1 ratio and centrifuged at 800 g at 4°C for 5 min to collect hemocytes. Cell lysis buffer for western blot analysis and IP were used to lyse hemocytes. After full lysis, the samples were centrifuged at 10,000–14,000 g at 4°C for 10 min, and the supernatants were collected. Protein supernatants were separated through 12% SDS-PAGE and then transferred to nitrocellulose filter membranes. The subsequent western blot procedure followed a previously described method (35). Rabbit anti-astakine antiserum and anti-GAPDH were purchased from HuaAn Biotechnology Co. (Hangzhou, China). Horseradish peroxidase-conjugated goat anti-rabbit secondary antibody was purchased from Biotek Biotechnology Company (Hangzhou, China).

Statistical Analysis

Relative gene expression was calculated using the $2^{-\Delta\Delta CT}$ method. SPSS 19.0 software (IBM, Armonk, NY, USA) was used to analyze data. Statistical significance was determined using the Duncan multiple comparison test or one-way analysis of variance for two group comparisons. All data are presented as the mean \pm standard deviation of three independent experiments. In all cases, $P < 0.05$ was considered to be statistically significant.

RESULTS

miR-133 Expression Following *V. parahaemolyticus* or WSSV Challenge

To determine whether miR-133 is involved in the response of *S. paramamosain* to WSSV or *V. parahaemolyticus* infection, hemocytes of healthy, WSSV-infected, and *V. parahaemolyticus*-infected mud crabs were collected to measure the expression of miR-133. The expression of miR-133 in *S. paramamosain* was obviously up-regulated after *V. parahaemolyticus* infection (Figure 1A), and a similar result was detected after WSSV infection, especially at 36 and 48 h (Figure 1B). These results suggest that miR-133 has potential as a new strategy for treating and preventing WSSV and *V. parahaemolyticus* infections. However, the expression of miR-133 was reduced by WSSV infection at 24 h, and we speculate that WSSV had not completely invaded the cells at this time point.

Effect of miR-133 Knockdown on Expression of miR-133 and Immune-Related Genes

The expression of miR-133 in hemocytes from 24 to 48 h post-AMO-miR-133 treatment was inhibited significantly (Figure 2A). The expression of miR-133 in hemocytes did not differ significantly between the PBS group and the AMO-miR-133-scrambled group at 24 h (Figure 2B).

We evaluated the immune pathways by analyzing the expression of nine important genes (*β -actin*, *STAT*, *astakine*, *MCM7*, *proPO*, *myosin*, *Toll-like receptor*, *CAP*, and *Relish*) after samples were treated with AMO-miR-133 for 24 h. Figure 2C shows the expression of immune-related genes in *S. paramamosain* at 24 h post-AMO-miR-133 treatment. The expression level of astakine increased significantly compared with that of the PBS group, and this finding was verified by SDS-PAGE (Figure 2D) and western blot analysis (Figure 2E). These results suggest that miR-133 might be involved in regulating the expression of astakine.

Effect of miR-133 Knockdown on CAT Activity

To evaluate the impact of miR-133 on CAT activity, we measured the CAT activity in hemocytes of *S. paramamosain*. After AMO-miR-133 treatment, the activities of CAT were significantly enhanced at different times (24, 36, and 48 h) compared with the PBS group (Figure 3A). The CAT activity of the WSSV + AMO-miR-133 group was higher than that of the WSSV group at 48 h (Figure 4A).

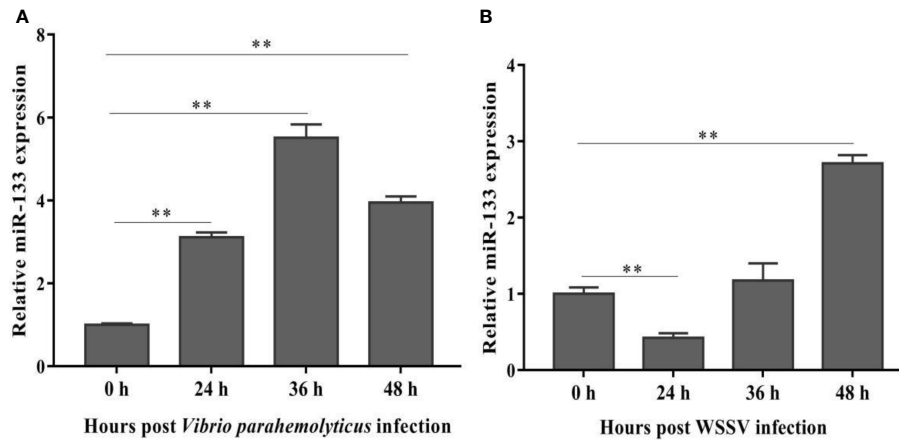


FIGURE 1 | *S. paramamosain* miR-133 expression following *V. parahaemolyticus* (A) (24 h $P = 0.0000080$, 36 h $P = 0.000019$, 48 h $P = 0.0000053$) or WSSV infection (B) (24 h $P = 0.00064$, 36 h $P = 0.29$, 48 h $P = 0.0048$) as measured using RT-qPCR. Hemocytes were collected at different times (0, 24, 36, 48 h) post challenge, and the miRNA of healthy, WSSV-infected or *V. parahaemolyticus*-infected mud crabs was extracted from hemocytes. Mud crab *GAPDH* was used as the control. Data presented were the mean \pm standard deviation of three independent experiments. Significant difference between different samples is indicated by $**P < 0.01$.

In contrast, the CAT activity of the *V. parahaemolyticus* + AMO-miR-133 group was reduced compared with that of the *V. parahaemolyticus* group at 36 and 48 h (Figure 4B).

Effect of miR-133 Knockdown on the THC

In the AMO-miR-133 group, the THC increased significantly from 24 to 48 h (Figure 3B), but the value at 48 h was significantly lower than that at 36 h. In the WSSV group, the THC decreased from 24 to 48 h (Figure 4C). However, in the WSSV + AMO-miR-133 group, the THC was significantly higher than that of the PBS and WSSV groups. *V. parahaemolyticus* challenge also showed the similar results (Figure 4D). These data indicate that miR-133 may affect hemocyte proliferation in *S. paramamosain*.

Effect of miR-133 Knockdown on SOD Activity

Significant differences in SOD activities were observed among the three groups at different times (24, 36 and 48 h) post-AMO-miR-133 treatment. For the AMO-miR-133 group, the SOD activity of crabs was significantly higher than that of the PBS group, especially at 24 h (Figure 3C). For the WSSV and *V. parahaemolyticus* groups, SOD activities were significantly enhanced at 24 h compared with the PBS group (Figure 4E). However, at 36 and 48 h, the SOD activity decreased in the *V. parahaemolyticus* group. In the WSSV group, the SOD activity was decreased (Figure 4F). The SOD activity of the WSSV + AMO-miR-133 group was higher than that of the WSSV group at 36 and 48 h post-challenge (Figure 4E). The *V. parahaemolyticus* challenge produced a similar result (Figure 4F).

Effect of miR-133 Knockdown on PO Activity

Compared to the PBS group, the PO activities of *S. paramamosain* treated with AMO-miR-133 were significantly lower from 24 to 48 h (Figure 3D). After WSSV or *V. parahaemolyticus* infection, the PO

activities of the two groups decreased significantly compared with that of the PBS group (Figures 4G, H). The PO activities of the AMO-miR-133 + WSSV and AMO-miR-133 + *V. parahaemolyticus* groups were higher than those of the WSSV or *V. parahaemolyticus* groups, respectively, from 24 to 36 h. However, the PO activities at 48 h were significantly lower than those at.

Effect of miR-133 Knockdown on ROS Activity and Hemocyte Proliferation

To evaluate the effect of miR-133 on hemocyte proliferation and ROS activity, we cultured *S. paramamosain* hemocytes in 96-well transparent plates and subsequently treated them with AMO-miR-133 or PBS. The ROS activity of the AMO-miR-133 group was significantly lower than that of the PBS group (Figures 5A–C), which echoed the results of SOD activity. The levels of hemocyte proliferation in the AMO-miR-133 group was higher than that of the PBS group at different times (24, 36, and 48 h) post-treatment (Figure 5D).

Effect of miR-133 Knockdown on Apoptosis

To assess how miR-133 affects hemocyte apoptosis, we measured the apoptosis rates in the AMO-miR-133 group. The hemocyte apoptosis rate was greatly up-regulated in the AMO-miR-133 group compared with the PBS group (Figures 6A, B). In response to WSSV or *V. parahaemolyticus* challenge, the apoptosis rates at 24 h were significantly higher than that of the PBS group (Figures 6C, E). After *V. parahaemolyticus* challenge, apoptosis rates were significantly enhanced in the *V. parahaemolyticus* + AMO-miR-133 group relative to the PBS group (Figure 6D), and similar results were obtained after WSSV challenge (Figure 6F). These results show that knockdown of miR-133 expression increased hemocyte apoptosis compared with that of healthy *S. paramamosain* and WSSV-infected (Figure 6H) or *V. parahaemolyticus*-infected crabs (Figure 6G).

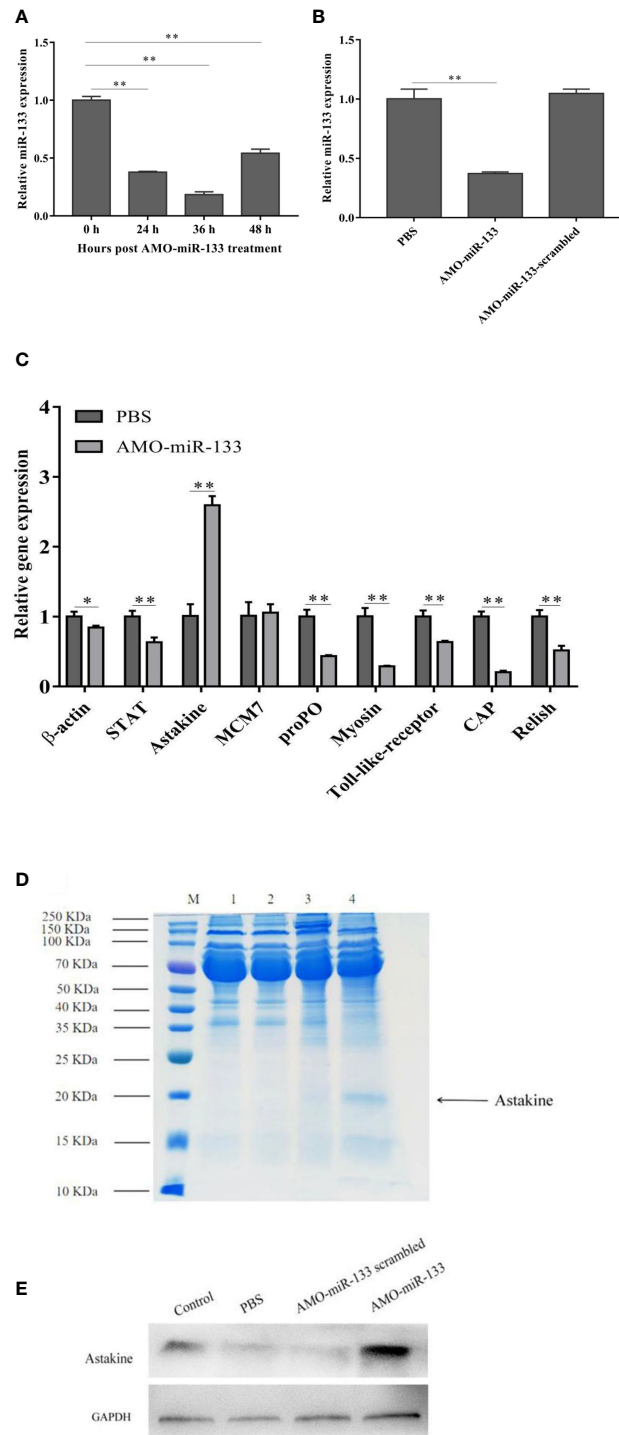


FIGURE 2 | Knockdown of miR-133. The miRNA of healthy, AMO-miR-133-scramble-treated or AMO-miR-133-treated *S. paramamosain* was extracted from hemocytes. **(A, B)** Expression levels of miR-133 in hemocytes of *S. paramamosain* detected by RT-qPCR, **(A)** (24 h $P = 0.000028$, 36 h $P = 0.000014$, 48 h $P = 0.00020$), **(B)** AMO-miR-133 $P = 0.000028$, AMO-miR-133 scrambled $P = 0.26$. **(C)** Relative expression of nine immune-related genes (β -actin ($P = 0.021$), STAT ($P = 0.0011$), astakine ($P = 0.00021$), MCM7 ($P = 0.75$), proPO ($P = 0.00053$), myosin ($P = 0.00050$), Toll-like receptor ($P = 0.00050$), CAP ($P = 0.000057$), Relish ($P = 0.0017$)) after AMO-miR-133 treatment. **(D)** Mud crabs were treated for 24 h with the indicated concentration of AMO-miR-133, then the cell lysate was prepared for SDS-PAGE (M: Marker; 1: Control; 2: PBS; 3: AMO-miR-133 scrambled; 4: AMO-miR-133) or **(E)** western blot analysis. Mud crab GAPDH was used as the control. Data presented were the mean \pm standard deviation of three independent experiments. Significant difference between different samples is indicated by * $P < 0.05$ and ** $P < 0.01$.

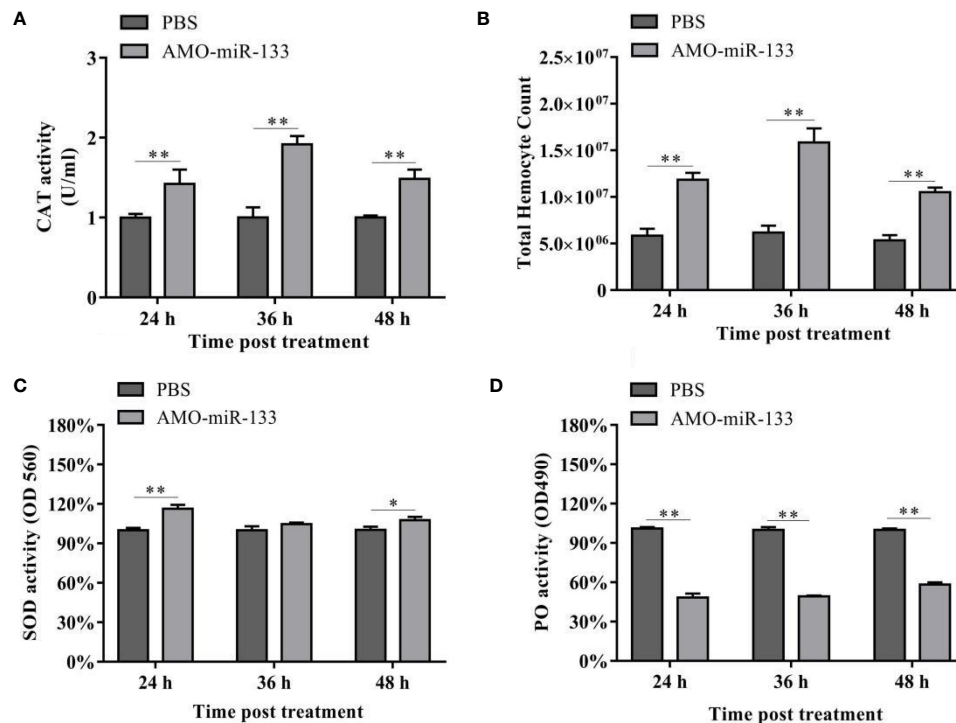


FIGURE 3 | (A) Effect of AMO-miR-133 on CAT activity of healthy *S. paramamosain* at 24, 36, and 48 h after AMO-miR-133 treatment. **(B)** Effect of AMO-miR-133 on the total hemocyte counts at 24, 36, and 48 h after AMO-miR-133 treatment. **(C)** Effect of AMO-miR-133 on SOD activity at 24, 36, and 48 h after AMO-miR-133 treatment. **(D)** Effect of AMO-miR-133 on PO activity at 24, 36, and 48 h after AMO-miR-133 treatment. The results are shown as mean \pm standard deviation of three independent experiments. Significant difference between different samples based on t-test analysis is indicated by * $P < 0.05$ and ** $P < 0.01$.

Effect of miR-133 Knockdown on Hemocyte Phagocytosis

To determine how miR-133 affects the phagocytosis of hemocytes, we investigated hemocyte phagocytosis in *S. paramamosain* at 24 h post-AMO-miR-133 treatment. The hemocyte phagocytic activity against WSSV and *V. parahaemolyticus* was enhanced compared with that of the PBS group (Figure 7).

Effect of miR-133 Knockdown on Virus Infection

To determine the function of miR-133 during WSSV infection, the virus copy numbers in *S. paramamosain* from the PBS group, WSSV group, and WSSV + AMO-miR-133 group were measured at different time after challenge (Figure 8A). At 24 h post-challenge, the virus copy number in the WSSV + AMO-miR-133 group was slightly lower than that of the WSSV group, but the difference was not statistically significant. From 48 to 72 h, the virus copy number in the WSSV + AMO-miR-133 group significantly increased relative to that of the WSSV group.

Effect of miR-133 Knockdown on Survival Rate

Figure 8B showed the cumulative survival rate of *S. paramamosain* from the PBS group, WSSV group, and WSSV + AMO-miR-133 group. A significantly higher mortality rate was found in the WSSV

+ AMO-miR-133 group compared with the WSSV group at 168 h post-infection. We obtained similar results after *V. parahaemolyticus* infection (Figure 8C). However, AMO-miR-133 itself had no adverse effects on *S. paramamosain*. These results suggest that miR-133 knockdown reduced the survival rate of WSSV-infected *S. paramamosain* or *V. parahaemolyticus*-infected *S. paramamosain*.

DISCUSSION

Although miRNAs have been implicated in the regulation of cell proliferation and signal transduction (3, 4) and are involved in numerous biological processes, their molecular functions are still largely unknown. Moreover, few studies of the roles of miRNAs in crustaceans have been conducted. Among crustaceans, miRNAs were first studied in *Daphnia pulex*, which is often used as a model animal (36). Crustaceans rely on innate immunity to protect themselves from invading microbes (37). For example, the hard carapace is the first line of defense for crabs, and it provides an effective physical barrier (38). If the hard carapace fails to resist pathogens, innate immunity, which consists of humoral and cellular responses, is stimulated (39).

Antisense oligonucleotides (AMOs) have been used to silence specific miRNAs *in vivo* in order to investigate the function of

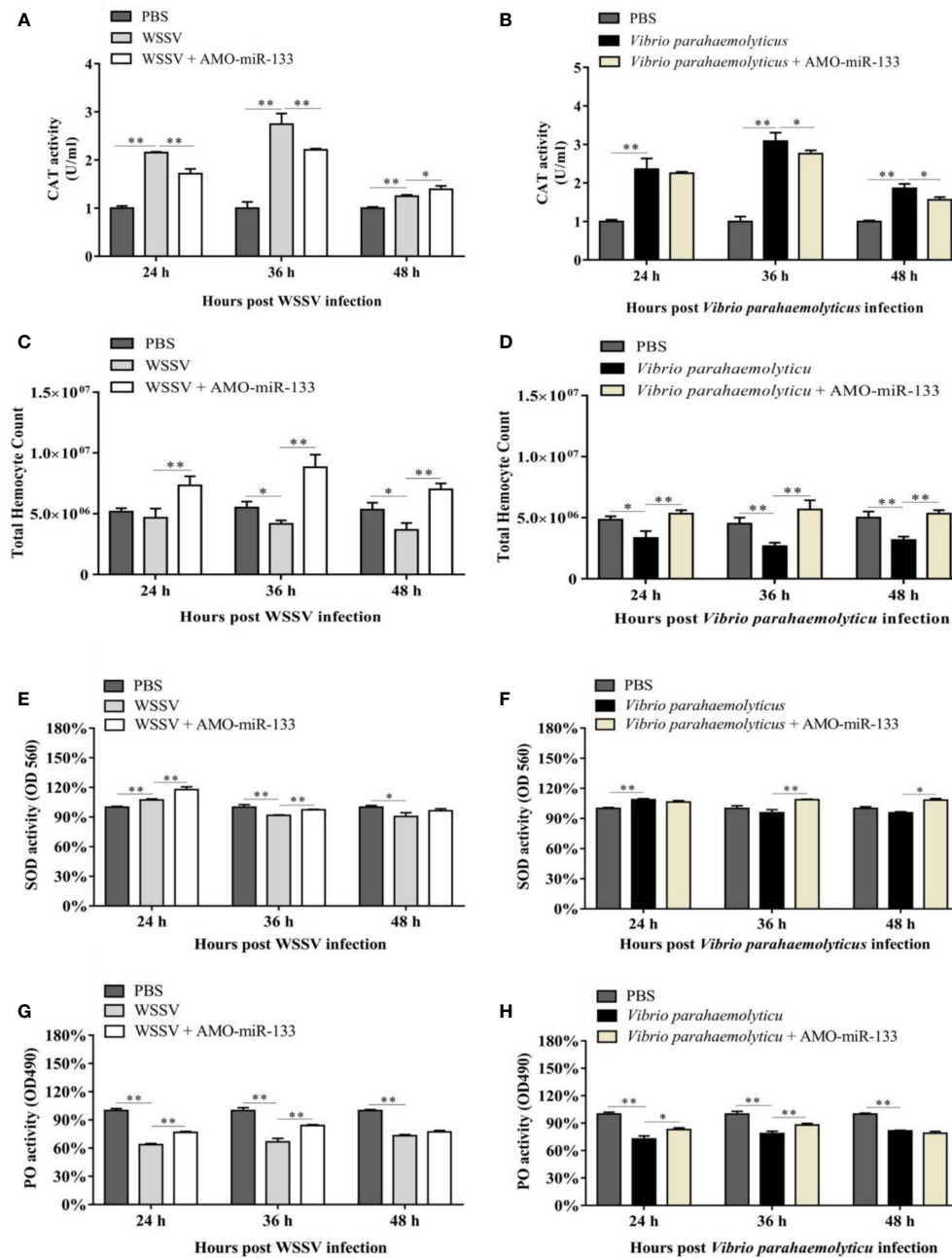


FIGURE 4 | Samples were taken at different times (24, 36, and 48 h) post-treatment. **(A)** CAT activity in the WSSV (24 h $P = 0.0000023$, 36 h $P = 0.000046$ and 48 h $P = 0.00035$) or WSSV + AMO-miR-133 group (24 h $P = 0.0017$, 36 h $P = 0.00062$ and 48 h $P = 0.033$). **(B)** CAT activity in the *V. parahaemolyticus* (24 h $P = 0.0012$, 36 h $P = 0.000065$ and 48 h $P = 0.00025$) or *V. parahaemolyticus* + AMO-miR-133 group (24 h $P = 0.55$, 36 h $P = 0.031$ and 48 h $P = 0.020$). **(C)** Effect of AMO-miR-133 on THC of WSSV-challenged mud crabs. WSSV group (24 h $P = 0.35$, 36 h $P = 0.016$ and 48 h $P = 0.024$). WSSV + AMO-miR-133 group (24 h $P = 0.0031$, 36 h $P = 0.0017$ and 48 h $P = 0.001641289$). **(D)** The effect of AMO-miR-133 on THC of *V. parahaemolyticus*-challenged mud crabs. *V. parahaemolyticus* group (24 h $P = 0.016$, 36 h $P = 0.0053$ and 48 h $P = 0.0053$). *V. parahaemolyticus* + AMO-miR-133 group (24 h $P = 0.0058$, 36 h $P = 0.0031$ and 48 h $P = 0.00078$). **(E)** SOD activity in the WSSV (24 h $P = 0.0013$, 36 h $P = 0.0046$ and 48 h $P = 0.021$) or WSSV + AMO-miR-133 group (24 h $P = 0.0043$, 36 h $P = 0.000052$ and 48 h $P = 0.079$). **(F)** SOD activity in the *V. parahaemolyticus* (24 h $P = 0.00086$, 36 h $P = 0.14$ and 48 h $P = 0.055$) or *V. parahaemolyticus* + AMO-miR-133 groups (24 h $P = 0.078$, 36 h $P = 0.0022$ and 48 h $P = 0.018$). **(G)** PO activity after WSSV or WSSV + AMO-miR-133 challenge. WSSV group (24 h $P = 0.0000096$, 36 h $P = 0.00029$ and 48 h $P = 0.0023$). WSSV + AMO-miR-133 group (24 h $P = 0.00031$, 36 h $P = 0.0023$ and 48 h $P = 0.15$). **(H)** PO activity after *V. parahaemolyticus* or *V. parahaemolyticus* + AMO-miR-133 treatment. *V. parahaemolyticus* group (24 h $P = 0.00029$, 36 h $P = 0.00067$ and 48 h $P = 0.000021$). *V. parahaemolyticus* + AMO-miR-133 group (24 h $P = 0.010$, 36 h $P = 0.0080$ and 48 h $P = 0.069$). The results are shown as mean \pm standard deviation of three independent experiments. Significant difference between different samples is indicated by * $P < 0.05$ and ** $P < 0.01$.

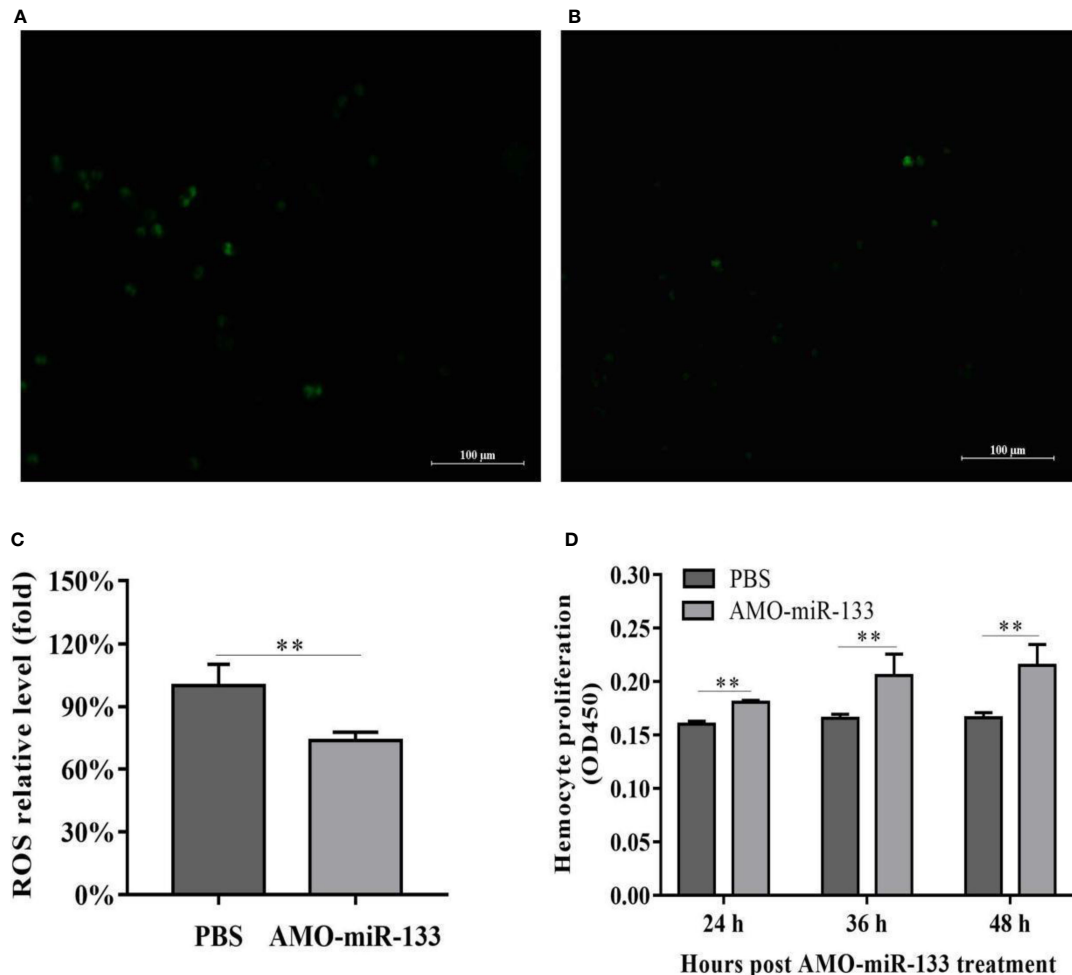


FIGURE 5 | ROS activity and proliferation of hemocytes. **(A)** PBS group. **(B)** AMO-miR-133 group. **(C)** ROS activity columnar statistical chart. **(D)** Hemocyte proliferation columnar statistical chart. Bars represent the means of three individual means \pm SD. Significant difference between different samples is indicated by $**P < 0.01$.

miRNAs in crustaceans (40, 41). Recent reports have shown that some miRNAs may play a major role in inhibiting virus invasion in mammals, and knockdown of miRNAs can increase the sensitivity of hosts to viral infection (42, 43). A variety of evidence has shown that miRNAs play an important role in the interaction between virus and host. Host miRNA can affect the replication and transmission of virus in the host by targeting virus or host genes, and a single miRNA often has multiple targeted genes (43).

To date, the study of miR-133 in the process of viral infection of hosts has mostly focused on mammals. Compared with vertebrates, few studies of the roles of miRNAs in the invertebrate response to virus infection have been reported (41). Mammal miR-133 was initially isolated from muscle cells and was later found to be involved in different physiological processes (44). For a long time, miR-133 was regarded as a muscle-specific miRNA, which may participate in myogenic diseases and regulate myoblast differentiation (45, 46). *In vitro*, miR-133 was shown to inhibit cardiac hypertrophy (47), and in a

variety of cancers, it was reported to suppress cell proliferation, apoptosis, and migration (17, 48, 49).

The mud crab *S. paramamosain* has become an economically important aquaculture species in southern and eastern China (50), but it is negatively impacted by diseases. Because miRNAs may have a potential antiviral role in viral infection, crustacean miRNAs need to be studied. A previous study performed using RT-qPCR technology to detect the change of miRNA expression in mud crabs infected with WSSV revealed that miR-133 was up-regulated in response to WSSV infection at 2 and 12 h post-infection (23). Thus, we choose miR-133 for further study.

The expression of mud crab miR-133 was significantly higher in hemocytes of WSSV-challenged crabs than in healthy crabs. This result suggests that mud crab miR-133 may participate in innate immunity and defend against WSSV or *V. parahaemolyticus* infection. To evaluate the potential function of miR-133 in the innate immune system of mud crabs, we examined the effect of AMO-miR-133 on immune-related gene expression, the survival of WSSV- or *V. parahaemolyticus*-challenged crabs, and other

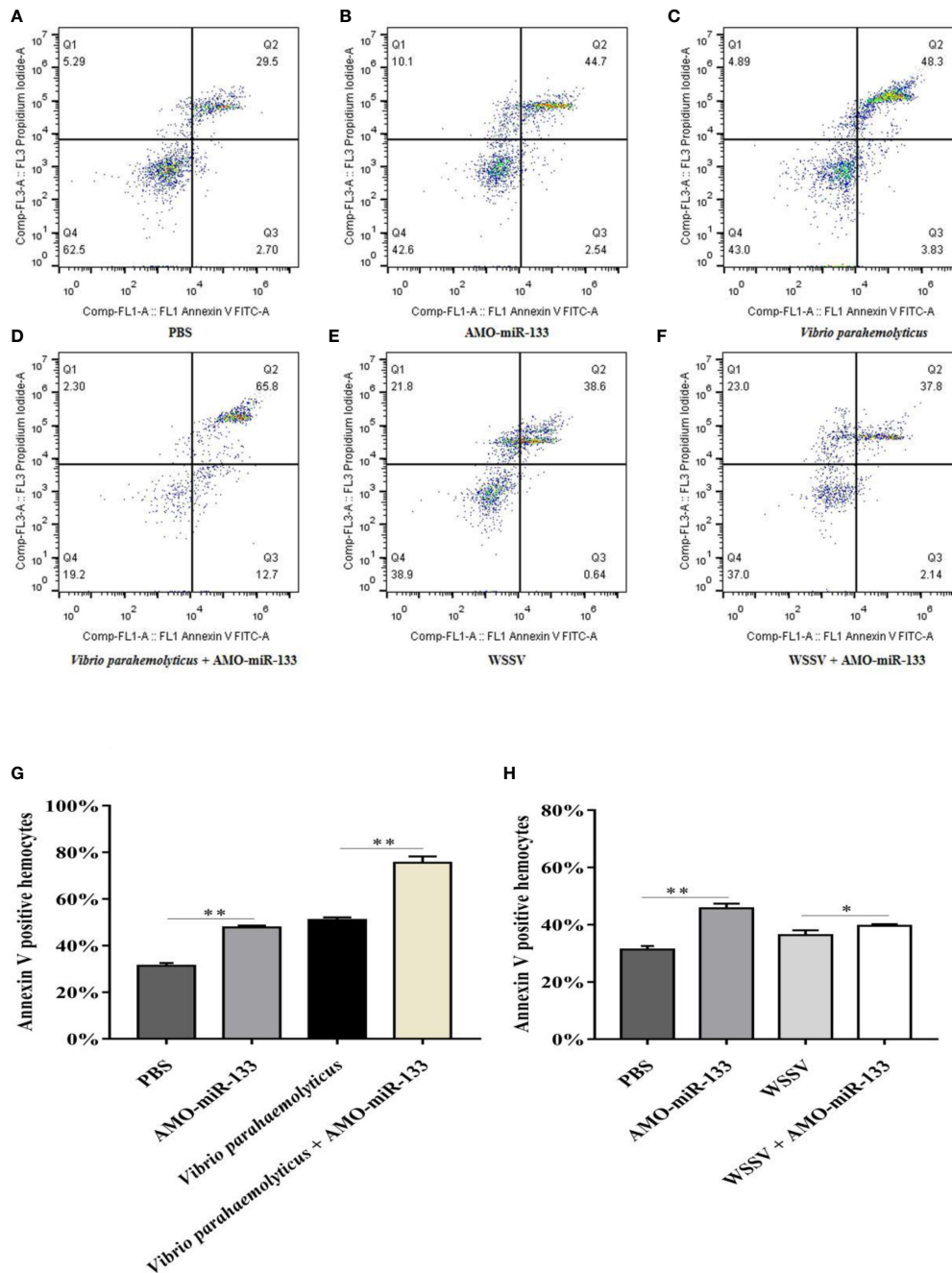
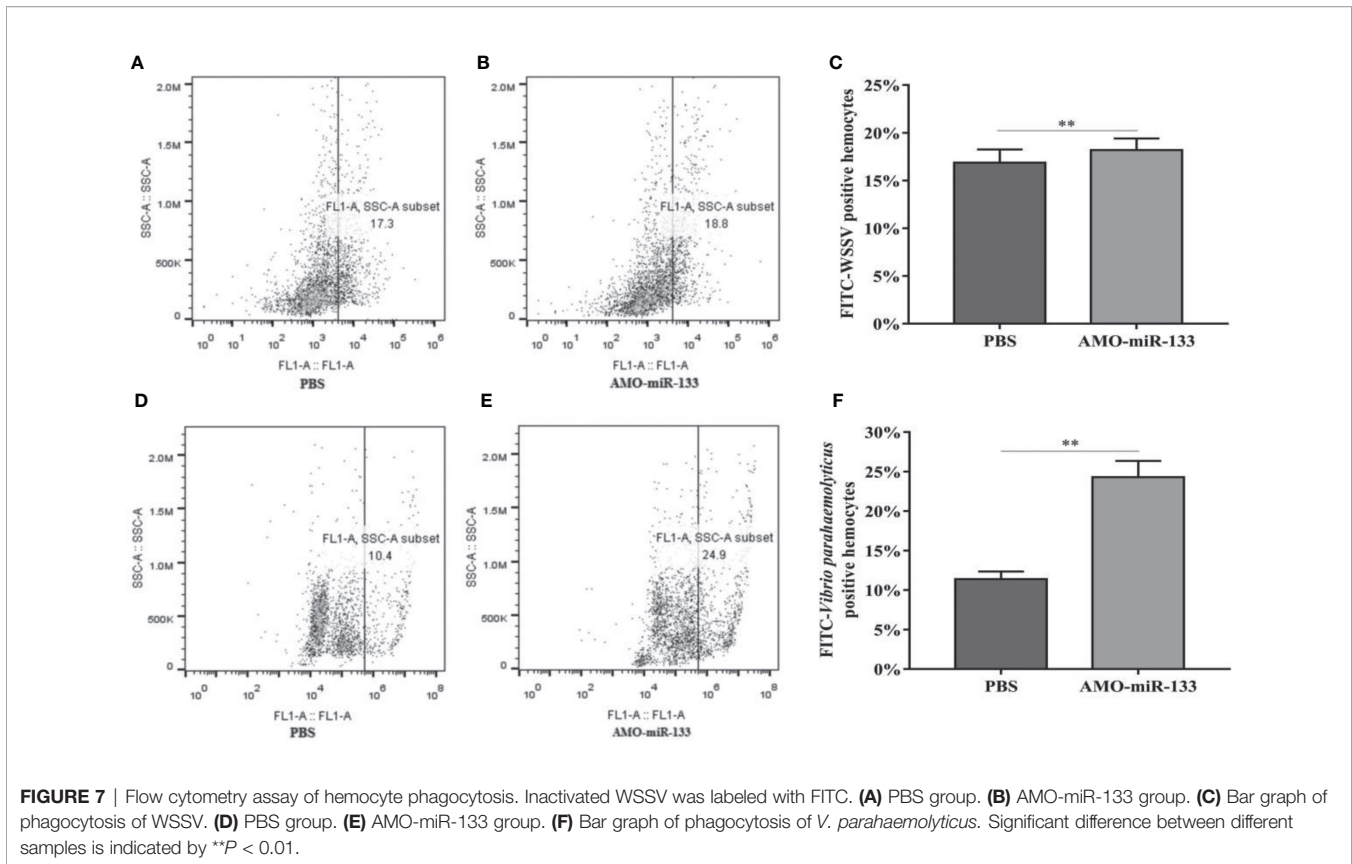


FIGURE 6 | Hemocyte apoptosis assay. (A) PBS group. (B) AMO-miR-133 group. (C) *V. parahaemolyticus* group. (D) *V. parahaemolyticus* + AMO-miR-133 group. (E) WSSV group. (F) WSSV + AMO-miR-133 group. (G) Bar graph of apoptosis after challenge with *V. parahaemolyticus*. (H) Statistical bar graph of apoptosis caused by WSSV infection. Significant difference between different samples is indicated by * $P < 0.05$ and ** $P < 0.01$.

immune-related parameters. Several immune-related genes related to pattern recognition receptors and signaling pathways have been reported (51–55). For example, the JAK/STAT signaling pathway was found to be important for vertebrate and invertebrate defense against viral infection (55, 56). The STAT gene, which is a major component of the JAK/STAT pathway, was identified in *Penaeus monodon*, *F. chinensis* and *S. paramamosain* (57, 58). Astakine is an

important hematopoietic cytokine that is directly involved in hematopoiesis, and it plays a major role in proliferation and differentiation of hematopoietic stem cells (59, 60). In a previous study, we found that crab MCM7 may contribute to the immune response to WSSV or *V. alginolyticus* infection by regulating phagocytosis, apoptosis, and other immune parameters (61). Myosin was also shown to be involved in antiviral defense and



cell skeleton construction in shrimp (62). Additionally, cationic antimicrobial peptide (CAP) in crabs can trigger host innate immunity against microbial invasion (63), and the antimicrobial peptide transcription factor Relish can regulate apoptosis in WSSV-infected *S. paramamosain* (52).

In this study, we used AMO-miR-133 to inhibit the expression of miR-133 in *S. paramamosain*. The expression levels of innate immune factors β -actin, STAT, proPO, myosin, Toll-like receptor, CAP, and Relish were significantly down-regulated after the knockdown of miR-133 in *S. paramamosain*, whereas that of *astakine* was up-regulated significantly. These results indicate that miR-133 may participate in immune regulation of mud crabs. Additionally, several immune parameters were detected in AMO-miR-133-treated *S. paramamosain*, which may help us understand the immune function of miR-133. THC increased significantly in the AMO-miR-133 group, and the increase was also found in the *in vitro* hemocyte proliferation experiments. This increase may be related to the up-regulation of *astakine* expression, as *astakine* was shown to induce a strong hematopoiesis response in crayfish (59). When we explored the function of *astakine* in mud crabs, we found that its expression was highest in hemocytes. After interfering with its expression, THC and cell proliferation were significantly reduced, which indicated that *astakine* affected hemocyte proliferation in the crabs (28).

High ROS levels lead to immune dysfunction, which is detrimental to aerobic organisms, and enzymatic and non-enzymatic antioxidants are used to scavenge redundant ROS (64,

65). Hydrogen peroxide can be catalyzed effectively by CAT, which helps maintain balance of its generation and efficient elimination (66). In our study, CAT and SOD activities were enhanced in the AMO-miR-133 group and in pathogen-challenged crabs, which suggests that knockdown of miR-133 improved the antioxidant capacity of the crabs. The ROS results confirmed this conclusion.

PO is important for the host immune response to several pathogens (67). We found that PO activity was down-regulated in AMO-miR-133-treated crabs, which suggests that miR-133 may participate in the immune response to WSSV or *V. parahaemolyticus* infection by regulating PO activity. The improved immune functional parameters in AMO-miR-133-treated crabs may be related to the up-regulation of *astakine*. We detected higher hemocyte apoptosis in the WSSV and *V. parahaemolyticus* groups than in the PBS group, and the WSSV + AMO-miR-133 and *V. parahaemolyticus* + AMO-miR-133 groups had higher hemocyte apoptosis than the WSSV or *V. parahaemolyticus* groups. Similarly, knocking down miR-133 improved hemocyte phagocytic activity in the immune response to WSSV or *V. parahaemolyticus* infection. These data suggest that miR-133 may participate in the immune response to WSSV or *V. parahaemolyticus* infection by affecting hemocyte apoptosis and phagocytosis. Similar findings were reported previously for MCM7 and Relish in *S. paramamosain* (52, 61). The higher number of virus copies and greater mortality observed in the WSSV + AMO-miR-133 group indicated that miR-133 may be involved in inhibiting WSSV replication. We also recorded higher mortality in the *V. parahaemolyticus* + AMO-miR-133 group during *V. parahaemolyticus* challenge.

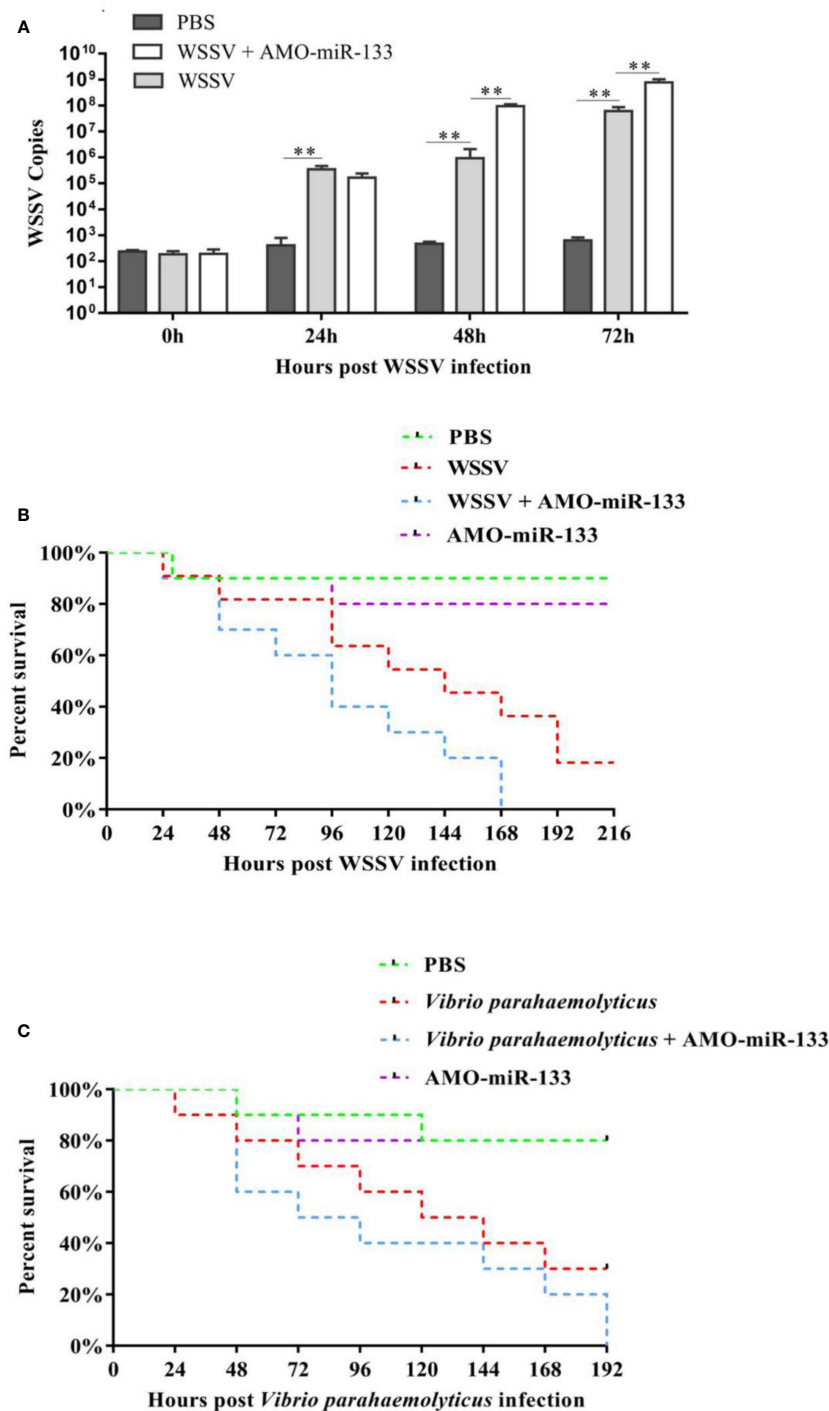


FIGURE 8 | (A) To analyze WSSV copies after WSSV challenge, hemocytes were collected at different times (0, 24, 48, 72 h) post-WSSV infection and assessed using RT-qPCR. **(B)** Cumulative mortality of WSSV- or **(C)** *V. parahaemolyticus*-challenged *S. paramamosain* treated with AMO-miR-133. Each group contained 10 individuals. Significant difference between different samples is indicated by ** $P < 0.01$.

In conclusion, our data suggest that miR-133 plays an important role in the innate immunity of *S. paramamosain*. miR-133 Knockdown enhanced the apoptosis or phagocytosis of crab hemocytes and increased the mortality of mud crabs after

WSSV or *V. parahaemolyticus* infection. Based on the results, miR-133 most likely affects innate immunity of mud crabs especially in hemocyte proliferation by regulating *astakine* expression. When mud crabs are infected with WSSV or *V.*

parahaemolyticus, miR-133 may change *astakine* expression to cope with pathogen infection. During this process, some important immune parameters, such as ROS, hemocyte apoptosis, and CAT and PO activities are affected by miR-133.

DATA AVAILABILITY STATEMENT

The original contributions presented in the study are included in the article/**Supplementary Material**. Further inquiries can be directed to the corresponding author.

AUTHOR CONTRIBUTIONS

We have made substantial contributions to the conception or design of the work; or the acquisition, analysis, or interpretation of data for the work. FZ and YZ conceived and designed research. YZ, YL, and XZ conducted experiments. FZ and YZ analyzed data. FZ and YZ wrote the manuscript. The corresponding author is responsible for ensuring that the descriptions are accurate and agreed by all authors. We have drafted the work or revised it critically for important intellectual content. We have

approved the final version to be published. We agree to be accountable for all aspects of the work in ensuring that questions related to the accuracy or integrity of any part of the work are appropriately investigated and resolved. YZ: Investigation, Data curation, Writing-Original draft preparation, Validation, Software. YL: Investigation, Sample preparation, Software. XZ: Investigation, Sample preparation. FZ: Conceptualization, Data curation, Writing-Reviewing and Editing. All authors contributed to the article and approved the submitted version.

FUNDING

This work was financially supported by Basic Public Welfare Research Project of Zhejiang Province (LY20C190001).

SUPPLEMENTARY MATERIAL

The Supplementary Material for this article can be found online at: <https://www.frontiersin.org/articles/10.3389/fimmu.2021.812717/full#supplementary-material>

REFERENCES

- Wang J, Sen S. MicroRNA Functional Network in Pancreatic Cancer: From Biology to Biomarker of Disease. *J Biosci* (2011) 36(3):481–91. doi: 10.1007/s12038-011-9083-4
- Treiber T, Treiber N, Meister G. Regulation of microRNA Biogenesis and Its Crosstalk With Other Cellular Pathways. *Nat Rev Mol Cell Biol* (2019) 20(1):5–20. doi: 10.1038/s41580-018-0059-1
- Bartel DP. MicroRNAs: Target Recognition and Regulatory Functions. *Cell* (2009) 136(2):215–33. doi: 10.1016/j.cell.2009.01.002
- Kozomara A, Birgaoanu M, Griffiths-Jones S. Mirbase: From microRNA Sequences to Function. *Nucleic Acids Res* (2019) 47(D1):D155–62. doi: 10.1093/nar/gky1141
- Li SK, Zhu S, Li CB, Zhang Z, Zhou L, Wang S, et al. Characterization of microRNAs in Mud Crab *Scylla Paramamosain* Under *Vibrio Parahaemolyticus* Infection. *PLoS One* (2013) 8(8):e73392. doi: 10.1371/journal.pone.0073392
- Zheng ZH, Aweya JJ, Wang F, Yao D, Lun J, Li S, et al. Acute Hepato-Pancreatic Necrosis Disease (AHPND) Related microRNAs in *Litopenaeus Vannamei* Infected With AHPND-causing Strain of *Vibrio Parahaemolyticus*. *BMC Genomics* (2018) 19:335. doi: 10.1186/s12864-018-4728-4
- Zhu F, Wang Z, Sun BZ. Differential Expression of microRNAs in Shrimp *Marsupenaeus Japonicus* in Response to *Vibrio Alginolyticus* Infection. *Dev Comp Immunol* (2016) 55:76–9. doi: 10.1016/j.dci.2015.10.012
- Huang Y, Wang W, Xu ZQ, Pan J, Zhao Z, Ren Q. *Eriocheir Sinensis* microRNA-7 Targets Crab Myd88 to Enhance White Spot Syndrome Virus Replication. *Fish Shellfish Immunol* (2018) 79:274–83. doi: 10.1016/j.dci.2015.10.012
- Huang Y, Han KK, Wang W, Ren Q. Host microRNA-217 Promotes White Spot Syndrome Virus Infection by Targeting Tube in the Chinese Mitten Crab (*Eriocheir Sinensis*). *Front Cell Infect Microbiol* (2017) 7:164. doi: 10.3389/fcimb.2017.00164
- Li X, Meng X, Luo K, Luan S, Shi X, Cao B, et al. The Identification of microRNAs Involved in the Response of Chinese Shrimp *Fenneropenaeus Chinensis* to White Spot Syndrome Virus Infection. *Fish Shellfish Immunol* (2017) 68:220–31. doi: 10.1016/j.fsi.2017.05.060
- Tang L, Wang H, Wang C, Mu C, Wei H, Yao H, et al. Temperature Potentially Induced Distinctive Flavor of Mud Crab *Scylla Paramamosain* Mediated by Gut Microbiota. *Sci Rep* (2020) 10(1):3720. doi: 10.1038/s41598-020-60685-0
- F.B.O.T. *China Fishery Yearbook*. Beijing (China: China agriculture press (2019).
- Lin X, Soderhall I. Crustacean Hematopoiesis and the Astakine Cytokines. *Blood* (2011) 117(24):6417–24. doi: 10.1182/blood-2010-11-320614
- Söderhäll K, Smith VJ. Separation of the Haemocyte Populations of *Carcinus Maenas* and Other Marine Decapods, and Phenoloxidase Distribution. *Dev Comp Immunol* (1983) 7(2):229–39. doi: 10.1016/0145-305X(83)90004-6
- Johansson M, Keyser P, Sritunyalucksana K, Soderhall K. Crustacean Haemocytes and Hematopoiesis. *Aquaculture* (2000) 191(1):45–52. doi: 10.1016/S0044-8486(00)00418-X
- Chen J, Mandel E, Thomson J, Wu Q, Callis TE, Hammond SM, et al. The Role of microRNA-1 and microRNA-133 in Skeletal Muscle Proliferation and Differentiation. *Nat Genet* (2006) 38(2):228–33. doi: 10.1038/ng1725
- Huang T, Zhu M, Li X, Zhao SH. Discovery of Porcine microRNAs and Profiling From Skeletal Muscle Tissues During Development. *PLoS One* (2008) 3(9):e3225. doi: 10.1371/journal.pone.0003225
- Yin V, Lepilina A, Smith A, Poss KD. Regulation of Zebrafish Heart Regeneration by miR-133. *Dev Biol* (2012) 365(2):319–27. doi: 10.1016/j.ydbio.2012.02.018
- Kogure T, Kondo Y, Ninomiya M, Nakagome Y, Kimura O, Iwata T, et al. MicroRNA-133b Plays an Onco-Suppressive Role in Hepatocellular Carcinoma. *Gastroenterology* (2014) 146(5):S–953. doi: 10.1016/S0016-5085(14)63466-1
- Tao J, Wu D, Xu B, Qian W, Li P, Lu Q, et al. MicroRNA-133 Inhibits Cell Proliferation, Migration and Invasion in Prostate Cancer Cells by Targeting the Epidermal Growth Factor Receptor. *Oncol Rep* (2012) 27(6):1967. doi: 10.3892/or.2012.1711
- Abdellatif M. The Role of microRNA-133 in Cardiac Hypertrophy Uncovered. *Circ Res* (2010) 106(1):16–8. doi: 10.1161/CIRCRESAHA.109.212183
- Li W, Liu M, Zhao C, Chen C, Kong Q, Cai Z, et al. MiR-1/133 Attenuates Cardiomyocyte Apoptosis and Electrical Remodeling in Mice With Viral Myocarditis. *Cardiol J* (2020) 27(3):285–94. doi: 10.5603/CJ.a2019.0036
- Lai YY, Jin QR, Zhu F. Differential Expression of microRNAs in Mud Crab *Scylla Paramamosain* in Response to White Spot Syndrome Virus (WSSV) Infection. *Fish Shellfish Immunol* (2020) 105:1–7. doi: 10.1016/j.fsi.2020.06.055
- Jin QR, Tian GY, Wu J, Jiang HL, Zhu F. Identification and Characterization of Hemocyte microRNAs in Mud Crab *Scylla Paramamosain* in Response to *Vibrio Parahaemolyticus* Infection. *Aquaculture* (2020) 524:735288. doi: 10.1016/j.aquaculture.2020.735288

25. Tassanakajon A, Somboonwiwat K, Supungul P, Tang S. Discovery of Immune Molecules and Their Crucial Functions in Shrimp Immunity. *Fish Shellfish Immunol* (2013) 34(4):954–67. doi: 10.1016/j.fsi.2012.09.021
26. Xiao C, Zhang Y, Zhu F. Effect of Dietary Sodium Butyrate on the Innate Immune Response of *Procambarus Clarkii* and Disease Resistance Against White Spot Syndrome Virus. *Aquaculture* (2021) 541:736784. doi: 10.1016/J.AQUACULTURE.2021.736784
27. Cheng C, Ma H, Deng Y, Feng J, Jie YK, Guo ZX. Effects of *Vibrio Parahaemolyticus* Infection on Physiological Response, Histopathology and Transcriptome Changes in the Mud Crab (*Scylla Paramamosain*). *Fish & Shellfish Immunol* (2019) 94:434–46. doi: 10.1016/j.fsi.2020.07.061
28. Wang J, Hong WJ, Zhu F. The Role of Astakine in *Scylla Paramamosain* Against *Vibrio Alginolyticus* and White Spot Syndrome Virus Infection. *Fish Shellfish Immunol* (2020) 98:236–44. doi: 10.1016/j.fsi.2020.01.024
29. Ma X, Sun B, Zhu F. Molecular Cloning of Kuruma Shrimp *Marsupenaeus Japonicus* Endonuclease-Reverse Transcriptase and Its Positive Role in White Spot Syndrome Virus and *Vibrio Alginolyticus* Infection. *Fish Shellfish Immunol* (2018) 73:297–308. doi: 10.1016/j.fsi.2017.12.031
30. Sun B, Qian X, Zhu F. Molecular Characterization of Shrimp Harbinger Transposase Derived 1 (HARB1)-Like and Its Role in White Spot Syndrome Virus and *Vibrio Alginolyticus* Infection. *Fish & Shellfish Immunol* (2018) 78:222–3. doi: 10.1016/j.fsi.2018.04.032
31. Qian X, Lai Y, Zhu F. Molecular Characterization of Carb Oxyptidase B-Like (CPB) in *Scylla Paramamosain* and Its Role in White Spot Syndrome Virus and *Vibrio Alginolyticus* Infection. *Fish Shellfish Immunol* (2019) 94:434–46. doi: 10.1016/j.fsi.2019.09.036
32. Musthafa MS, Ali AJ, Ali AH, Hyder Ali AR, Mohamed MJ, War M, et al. Effect of Shilajit Enriched Diet on Immunity, Antioxidants, and Disease Resistance in *Macrobrachium Rosenbergii* (De Man) Against *Aeromonas Hydrophila*. *Fish & Shellfish Immunol* (2016) 57:293–300. doi: 10.1016/j.fsi.2016.08.033
33. Zhang Y, Wu J, Xu W, Gao J, Cao H, Yang M, et al. Cytotoxic Effects of Avermectin on Human HepG2 Cells *In Vitro* Bioassays. *Environ Pollution* (2017) 220:1127–37. doi: 10.1016/j.envpol.2016.11.022
34. Wang Z, Zhu F. MicroRNA-100 is Involved in Shrimp Immune Response to White Spot Syndrome Virus (WSSV) and *Vibrio Alginolyticus* Infection. *Sci Rep* (2017) 7:42334. doi: 10.1038/srep42334
35. Liu LK, Gao RL, Gao Y, Xu JY, Guo LM, Wang KJ, et al. A Histone K-Lysine Acetyltransferase CqKAT2A-Like Gene Promotes White Spot Syndrome Virus Infection by Enhancing Histone H3 Acetylation in Red Claw Crayfish *Cherax Quadricarinatus*. *Dev Comp Immunol* (2020) 107:103640. doi: 10.1016/j.dci.2020.103640
36. Wheeler BM, Heimberg AM, Moy VN, Sperling EA, Holstein TW, Heber S, et al. The Deep Evolution of Metazoan microRNAs. *Evol Dev* (2009) 11(1):50–68. doi: 10.1111/j.1525-142X.2008.00302.x
37. Vazquez L, Alpuche J, Maldonado G, Agundis C, Pereyra-Morales A, Zenteno E, et al. Review: Immunity Mechanisms in Crustaceans. *Innate Immun* (2009) 15(3):179–88. doi: 10.1177/1753425909102876
38. Chen F, Wang K. Characterization of the Innate Immunity in the Mud Crab *Scylla Paramamosain*. *Fish Shellfish Immunol* (2019) 93:436–48. doi: 10.1016/j.fsi.2019.07.076
39. Jiravanichpaisal P, Lee B, Söderhäll K. Cell-Mediated Immunity in Arthropods: Hematopoiesis, Coagulation, Melanization and Oponization. *Immunobiology* (2006) 211(4):213–36. doi: 10.1016/j.imbio.2005.10.015
40. Wang Z, Zhu F. Different Roles of a Novel Shrimp microRNA in White Spot Syndrome Virus (WSSV) and *Vibrio Alginolyticus* Infection. *Dev Comp Immunol* (2017) 79:21–30. doi: 10.1016/j.dci.2017.10.002
41. Huang T, Zhang X. Functional Analysis of a Crustacean microRNA in Host-Virus Interactions. *J Virol* (2012) 86(23):12997. doi: 10.1128/JVI.01702-12
42. Ambros V. The Functions of Animal microRNAs. *Nature* (2004) 431(7006):350–5. doi: 10.1038/nature02871
43. Triboulet R, Mari B, Lin Y, Chable-Bessia C, Bannasser Y, Lebrigand K, et al. Suppression of microRNA-Silencing Pathway by HIV-1 During Virus Replication. *Science* (2007) 315(5818):1579–82. doi: 10.1126/science.1136319
44. Yu H, Lu Y, Li Z, Wang Q. MicroRNA-133: Expression, Function and Therapeutic Potential in Muscle Diseases and Cancer. *Curr Drug Targets* (2014) 15(9):817–28. doi: 10.2174/1389450115666140627104151
45. Rao PK, Missaglia E, Shields L, Hyde G, Yuan B, Shepherd CJ, et al. Distinct Roles for miR-1 and miR-133a in the Proliferation and Differentiation of Rhabdomyosarcoma Cells. *FASEB J* (2010) 24(9):3427–37. doi: 10.1096/fj.09-150698
46. Bostjancic E, Zidar N, Stajer D and Glavac D. MicroRNAs miR-1, miR-133a, miR-133b and miR-208 Are Dysregulated in Human Myocardial Infarction. *Cardiology* (2010) 115(3):163–9. doi: 10.1159/000268088
47. Ruizlozano PP. MicroRNA-133 Controls Cardiac Hypertrophy. *Nat Med* (2007) 13(5):613–8. doi: 10.1038/nm1582
48. Wang DS, Zhang HQ, Zhang B, Yuan ZB, Yu ZK, Yang T, et al. MiR-133 Inhibits Pituitary Tumor Cell Migration and Invasion via Down-Regulating FOXC1 Expression. *Genet Mol Res* (2016) 15(1):gmr7453. doi: 10.4238/gmr.15017453
49. Xu C, Lu Y, Pan Z, Chu W, Luo X, Lin H, et al. The Muscle-Specific microRNAs miR-1 and miR-133 Produce Opposing Effects on Apoptosis by Targeting HSP60, HSP70 and Caspase-9 in Cardiomyocytes. *J Cell Sci* (2007) 120:3045–52. doi: 10.1242/jcs.010728
50. Lin Z, Hao M, Huang Y, Zou W, Rong H, Wen X. Cloning, Tissue Distribution and Nutritional Regulation of a Fatty Acyl Elov4-Like Elongase in Mud Crab, *Scylla Paramamosain* (Estampador, 1949). *Comp Biochem Physiol B: Biochem Mol Biol* (2018) 217:70–8. doi: 10.1016/j.cbpb.2017.12.010
51. Deng H, Xu X, Hu L, Li J, Zhou D, Liu S, et al. A Janus Kinase From *Scylla Paramamosain* Activates JAK/STAT Signaling Pathway to Restrain Mud Crab Reovirus. *Fish Shellfish Immunol* (2019) 90:275–87. doi: 10.1016/j.fsi.2019.03.056
52. Zhu F, Sun BZ, Wang Z. The Crab Relish Plays an Important Role in White Spot Syndrome Virus and *Vibrio Alginolyticus* Infection. *Fish Shellfish Immunol* (2019) 87:297–306. doi: 10.1016/j.fsi.2019.01.028
53. Chen Y, Awewa J, Sun W, Wei X, Gong Y, Ma H, et al. SpToll1 and SpToll2 Modulate the Expression of Antimicrobial Peptides in *Scylla Paramamosain*. *Dev Comp Immunol* (2018) 87:124–36. doi: 10.1016/j.dci.2018.06.008
54. Takaoka A, Yanai H. Interferon Signalling Network in Innate Defence. *Cell Microbiol* (2006) 8(6):907–22. doi: 10.1111/j.1462-5822.2006.00716.x
55. Dostert C, Jouanguy E, Irving P, Troxler L, Galiana-Arnoux D, Hetru C, et al. The Jak-STAT Signaling Pathway is Required but Not Sufficient for the Antiviral Response of *Drosophila*. *Nat Immunol* (2005) 6(9):946. doi: 10.1038/ni1237
56. Chen W, Kun C, Jian H, Liu KF, Wang HC, Kou GH, et al. WSSV Infection Activates STAT in Shrimp. *Dev Comp Immunol* (2008) 32(10):1142–50. doi: 10.1016/j.dci.2008.03.003
57. Sun C, Shao H, Zhang X, Zhao X, Wang J. Molecular Cloning and Expression Analysis of Signal Transducer and Activator of Transcription (STAT) From the Chinese White Shrimp. *Fenneropenaeus chinensis Sociological Thought* (2011) 38:5313–9. doi: 10.1007/s11033-011-0681-x
58. Deng H, Zhang W, Li J, Li J, Hu L, Yan W, et al. A Signal Transducers and Activators of Transcription (STAT) Gene From *Scylla Paramamosain* is Involved in Resistance Against Mud Crab Reovirus. *Fish Shellfish Immunol* (2019) 94:580–91. doi: 10.1016/j.fsi.2019.09.045
59. Söderhäll I, Kim YA, Jiravanichpaisal P, Lee SY, Söderhäll K. An Ancient Role for a Prokineticin Domain in Invertebrate Hematopoiesis. *J Immunol* (2005) 174(10):6153–60. doi: 10.4049/jimmunol.174.10.6153
60. Söderhäll I. Crustacean Hematopoiesis. *Dev Comp Immunol* (2016) 58:129–41. doi: 10.1016/j.dci.2015.12.009
61. Zhu F, Qian X, Wang Z. Molecular Characterization of Minichromosome Maintenance Protein (MCM7) in *Scylla Paramamosain* and Its Role in White Spot Syndrome Virus and *Vibrio Alginolyticus* Infection. *Fish Shellfish Immunol* (2018) 83:104–14. doi: 10.1016/j.fsi.2018.09.028
62. Li C, Weng S, He J. WSSV-Host Interaction: Host Response and Immune Evasion. *Fish Shellfish Immunol* (2019) 84:558–71. doi: 10.1016/j.fsi.2018.10.043
63. Imjongjirak C, Amparyup P, Tassanakajon A, Sittipraneed S. Molecular Cloning and Characterization of Crustin From Mud Crab *Scylla Paramamosain*. *Mol Biol Rep* (2009) 36(5):841–50. doi: 10.1007/s11033-008-9253-0
64. Malhotra J, Kaufman R. Endoplasmic Reticulum Stress and Oxidative Stress: A Vicious Cycle or A Double-Edged Sword? *Antioxid Redox Signal* (2007) 9(12):2277–93. doi: 10.1089/ars.2007.1782
65. Cerutti PA. Prooxidant States and Tumor Promotion. *Science* (1985) 227:375–81. doi: 10.1126/science.2981433
66. Ha E, Oh C, Ryu J, Bae Y, Kang S, Jang IH, et al. An Antioxidant System Required for Host Protection Against Gut Infection in *Drosophila*. *Dev Cell* (2005) 8(1):125–32. doi: 10.1016/j.devcel.2004.11.007

67. Cerenius L, Lee BL, Soderhall K. The proPO-System: Pros and Cons for Its Role in Invertebrate Immunity. *Trends Immunol* (2008) 29:263–71. doi: 10.1016/j.it.2008.02.009

Conflict of Interest: The authors declare that the research was conducted in the absence of any commercial or financial relationships that could be construed as a potential conflict of interest.

Publisher's Note: All claims expressed in this article are solely those of the authors and do not necessarily represent those of their affiliated organizations, or those of

the publisher, the editors and the reviewers. Any product that may be evaluated in this article, or claim that may be made by its manufacturer, is not guaranteed or endorsed by the publisher.

Copyright © 2022 Zhang, Lai, Zhou and Zhu. This is an open-access article distributed under the terms of the Creative Commons Attribution License (CC BY). The use, distribution or reproduction in other forums is permitted, provided the original author(s) and the copyright owner(s) are credited and that the original publication in this journal is cited, in accordance with accepted academic practice. No use, distribution or reproduction is permitted which does not comply with these terms.